Journal of Inorganic Biochemistry xxx (2016) xxx–xxx

Contents lists available at ScienceDirect

Journal of Inorganic Biochemistry

journal homepage: www.elsevier.com/locate/jinorgbio

The in vitro antitumor activity of arene-ruthenium(II) curcuminoid complexes improves when decreasing curcumin polarity

Francesco Caruso [a,*], Riccardo Pettinari [b], Miriam Rossi [a], Elena Monti [c], Marzia Bruna Gariboldi [c], Fabio Marchetti [b], Claudio Pettinari [d], Alessio Caruso [a], Modukuri V. Ramani [e], Gottumukkala V. Subbaraju [e,*]

[a] Vassar College, Department of Chemistry, Poughkeepsie, NY 12604, USA
[b] School of Science and Technology, Università di Camerino, via S. Agostino 1, 62032 Camerino, MC, Italy
[c] University of Insubria, Department of Structural and Functional Biology, Via A. da Giussano 10, 21052, Busto Arsizio, Varese, Italy
[d] School of Pharmacy, Università di Camerino, via S. Agostino 1, 62032 Camerino, MC, Italy
[e] Natsol Laboratories Private Limited, Commercial Hub, J.N. Pharma City, Visakhapatnam 531019, India

ARTICLE INFO

Article history:
Received 20 September 2015
Received in revised form 21 May 2016
Accepted 3 June 2016
Available online xxxx

Keywords:
Ruthenium(II)
Modified curcumin
Liposolubility
Antiproliferative activity
<Beta>-diketone
Apoptosis

ABSTRACT

The antitumor activity of ruthenium(II) arene (*p*-cymene, benzene, hexamethylbenzene) derivatives containing modified curcumin ligands (HCurcI = (1E,4Z,6E)-5-hydroxy-1,7-bis(3,4-dimethoxyphenyl)hepta-1,4,6-trien-3-one and HCurcII = (1E,4Z,6E)-5-hydroxy-1,7-bis(4-methoxyphenyl)hepta-1,4,6-trien-3-one) is described. These have been characterized by IR, ESI-MS and NMR spectroscopy. The X-ray crystal structure of HCurcI has been determined and compared with its related Ru complex. Four complexes have been evaluated against five tumor cell lines, whose best activities [IC_{50} (μM)] are: breast MCF7, 9.7; ovarian A2780, 9.4; glioblastoma U-87, 9.4; lung carcinoma A549, 13.7 and colon-rectal HCT116, 15.5; they are associated with apoptotic features. These activities are improved when compared to the already known corresponding curcumin complex, (*p*-cymene)Ru(curcuminato)Cl, about twice for the breast and ovarian cancer, 4.7 times stronger in the lung cancer and about 6.6 times stronger in the glioblastoma cell lines. In fact, the less active (*p*-cymene)Ru(curcuminato)Cl complex only shows similar activity to two novel complexes in the colon cancer cell line. Comparing antitumor activity between these novel complexes and their related curcuminoids, improvement of antiproliferative activity is seen for a complex containing CurcII in A2780, A549 and U87 cell lines, whose IC_{50} are halved. Therefore, after replacing OH curcumin groups with OCH_3, the obtained species HCurcI and its Ru complexes have increased antitumor activity compared to curcumin and its related complex. In contrast, HCurcII is less cytotoxic than curcumin but its related complex [(*p*-cymene)Ru(CurcII)Cl] is twice as active as HCurcII in 3 cell lines. Results from these novel arene-Ru curcuminoid species suggest that their increased cytotoxicity on tumor cells correlate with increase of curcuminoid lipophilicity.

1. Introduction

Searching for new cancer chemotherapeutics is an ongoing significant process that encompasses contributions from different scientific disciplines. Although most new potential candidates are organic compounds, metal antitumor complexes increasingly are of interest due to the success of the well-established group of cisplatin derivatives. In this category only complexes having the low metal oxidation state, Pt^{II}, are currently in medicinal use, although both Pt^{II} and Pt^{IV} compounds can be antitumor active species. Evidence of Pt^{IV} to Pt^{II} reduction in compounds has been suggested in the literature, however, and this enriches possibilities for success in the search of new drugs.

A major group of currently investigated anticancer non-Pt metal agents includes Ru compounds [1–2]. In fact, two Ru^{III} species, NAMI-A (anti-metastatic) [3] and KP1019 [4] are in clinical trials [5]. The pioneering work of P. Sadler demonstrated that arene Ru^{II} complexes are also effective [6]. Such compounds in aqueous solution have similar ligand exchange kinetics as Pt^{II} complexes [7]. Arene-Ru^{II} ethylenediamine complexes show very high activity both in vitro and in vivo [8–10]. Antitumor arene ruthenium compounds have been the subject of several reviews [5,11–14], including a recent publication that contains an excellent historical perspective [15].

The mechanism of action of arene Ru^{II} antitumor compounds is not well understood even though their interaction with endogenous biological molecules has been studied. Reactions between (η^6-

* Corresponding authors.
E-mail addresses: caruso@vassar.edu (F. Caruso), subbarajugv@gmail.com (G.V. Subbaraju).

http://dx.doi.org/10.1016/j.jinorgbio.2016.06.002
0162-0134/

arene)Ru(ethylenediamine) species and DNA [16–18], serum proteins, peptides and amino acids [19–20], suggest that DNA is the favored target in living cells, specifically through metal binding at guanine N-7 [21]. DNA intercalation by these Ru^{II} complexes is also feasible, both by arene pendant flat moieties [22], and by an aromatic substituent in the chelating ligand [23]. However, a combination (DNA-protein) target interaction with the drug cannot be excluded since when arene-Ru-(alanine) is reacted with 9-ethylguanine, the mixed (DNA-base)-(amino acid) species, (η^6-benzene)Ru(alanine)(9-ethylguanine) is obtained [24].

The interactions of Ru-arene compounds with proteins [25–28] and glutathione [29] also have been studied and show that such targets are important for antitumor activity. The crystal structure of glycogen synthase kinase A shows a half-sandwich ruthenium complex at the ATP binding site A [30]. The localization in cancer cells of the relatively non-cytotoxic anti-metastatic compound [Ru(*p*-cymene)(1,3,5-triaza-7-phosphaadamantane)Cl_2] and the cytostatic [Ru(*p*-cymene)(ethylenediamine)Cl]PF_6 species have been recently explored using inductively coupled plasma mass spectrometry (ICP-MS) [31]. It was found that a protein target is indeed preferred for the former, as the complex reacts with histones. In contrast, the ethylenediamine complex is more active towards guanine bases, indicating that subtle structural changes in the Ru-arene complex can facilitate interactions with different targets.

The biological activity of Ru^{III} is believed to mimic that of Fe^{III} since the similar hardness and atomic radius for both cations make them indistinguishable in the binding to biomolecules. Furthermore, since cancer cells overexpress transferrin receptors to satisfy their increased demand for iron, Ru-based drugs may be delivered more efficiently to cancer cells than healthy ones [32]. Recent investigations, however, have established that transferrin smuggling of Ru^{II} in the cell occurs via a different pathway. The soft Ru^{II} species looks for other transferrin amino acids, which do not modify the "normal" conformation of Fe^{III} loaded transferrin [33] and seems to facilitate its passage through the cell membrane. Thus, it seems that although antitumor Ru^{III} complexes are able to effect a replacement of Fe^{III} in transferrin by Ru^{III} ions, Ru^{II} seeks alternate pathways with which to bind to protein targets. As a result, interestingly, the Ru^{II} complex may conserve part of its coordination environment, including the robust Ru-arene bond during hydrolysis.

Besides its intrinsic and unique properties, ruthenium can bind small molecules that already exhibit biological activity as ligands in its coordination sphere, thus preserving them from detoxification/deactivation in biological fluids. It seems that limited efforts have been made in conjugating the metal center with such ligands and so we are investigating the chemistry and potential antitumor activity of novel arene Ru^{II} complexes with structural variants of curcumin [34], a molecule showing remarkable anti-inflammatory, anti-angiogenic, anti-oxidant, wound healing and anti-cancer properties [35]. The use of curcumin, defined as the Indian solid gold [36], as a coordinating ligand is of interest in bioinorganic chemistry since it is edible in large amounts (up to 10 g daily) and innocuous.

Formation of the Ru-curcumin complex increases curcumin stability since on its own it is unstable in water. As a result, curcumin coordination to Ru assists in bringing the ligand to the appropriate biological target. The arene-Ru^{II} curcuminoid complexes we describe are closely related to the corresponding arene-Ru^{II} β-diketonato acetylacetonato species previously found to be active [37]. We report the chemical characterization and in vitro antitumor activity on 5 tumor cell lines of related complexes where the curcumin-like ligands are less polar than the parent compound. Other investigators have studied Ru complexes of curcumin modified at its aromatic rings by thiophene moieties [38], in contrast with our ligands that conserve the entire curcumin structural skeleton. Curcumin, HCurcI and HCurcII ligands also are studied in the same cell lines for comparison.

2. Experimental

2.1. Materials and methods

The dimers [Ru(η^6-arene)Cl_2]$_2$ (arene = *p*-cymene, benzene or hexamethylbenzene) were purchased from Aldrich and TCI Europe and used as received. The curcumin-derivative ligands HCurcI and HCurcII were synthesized as described below. All other materials were obtained from commercial sources and used as received. IR spectra were recorded from 4000 to 600 cm^{-1} on a Perkin-Elmer Spectrum 100 FT-IR instrument. ^1H and ^{13}C NMR spectra were recorded on a 400 Mercury Plus Varian instrument operating at room temperature (400 MHz for ^1H and 100 MHz for ^{13}C). Referencing is relative to TMS (^1H and ^{13}C). Positive and negative ion electrospray mass spectra were obtained with a Series 1100 MSI detector HP spectrometer, using an acetonitrile mobile phase. Solutions (3 mg/mL) for electrospray ionization mass spectrometry (ESI-MS) were prepared using reagent-grade acetonitrile. Mass and intensities were compared to those calculated using IsoPro Isotopic Abundance Simulator, version 2.1.28. Melting points are uncorrected and were taken on an STMP3 Stuart scientific instrument and on a capillary apparatus. Samples for microanalysis were dried in vacuo to constant weight (20 °C, ca. 0.1 Torr) and were performed on a Fisons Instruments 1108 CHNS-O elemental analyzer. Electrical conductivity measurements (Λ_M, reported as S cm^2 mol^{-1}) of acetonitrile and dichloromethane solutions of the complexes were recorded using a Crison CDTM 522 conductimeter at room temperature.

2.1.1. Synthesis of ligands related to curcumin

2.1.1.1. HCurcI, (1E,4Z,6E)-5-hydroxy-1,7-bis(3,4-dimethoxyphenyl)hepta-1,4,6-trien-3-one. To a solution of acetylacetone (6.6 mL, 0.0649 mol) in ethyl acetate (18 mL) was added 3,4-dimethoxybenzaldehyde - also known as methylvanillin or vertraldehyde (18 g, 0.1083 mol), trimethyl borate (31.3 mL, 0.281 mol) and *n*-butyl amine (1.59 mL, 0.0162 mol) at room temperature and the reaction mixture was heated to 65 °C and maintained at the same temperature for 6.0 h. After this period, the reaction mixture was cooled to room temperature and filtered. The reaction mass and the residue were transferred into a round bottom flask (0.5 L) and 10% acetic acid (180 mL) was added. The reaction mixture was heated to 110 °C and maintained for 5.0 h. Afterwards the reaction mass was cooled to room temperature and filtered; the residue obtained was transferred into a round bottom flask (0.5 L), and acetone (108 mL) was added, and the temperature slowly raised to 65 °C. Water (108 mL) was added dropwise and refluxed for 2 h, then the reaction mixture was cooled to room temperature and filtered. The obtained material was dried under vacuum for 2 h at 60 °C (14 g, 66% yield, HPLC purity: 97.86%). This is soluble in diethyl ether, alcohols, acetone, acetonitrile, DMSO, and chloro-hydrocarbon solvents. M.p. 132–133 °C. Anal. Calcd. for $C_{23}H_{24}O_6$: C, 69.68; H, 6.10. Found: C, 69.54; H, 5.96. IR (cm^{-1}): IR (cm^{-1}): 1618 m, 1695s, 1578s, 15080s ν(C═C, C═O). ^1H NMR ($CDCl_3$, 298 K): δ 3.93 (s, 12H, —OCH_3), 5.81 (s, 1H, C(1)H), 6.48 (d, 2H, C(3,3′)H, $^3J_{trans}$ = 15.6 Hz), 6.87 (m, 2H, C(9, 9′)H), 7.12 (m, 4H, C(10, 10′)H and C(6, 6′)H), 7.62 (d, 2H, C(4, 4′)H, $^3J_{trans}$ = 15.6 Hz). ^{13}C NMR ($CDCl_3$, 298 K): δ, 56.2 (s, O—CH_3), 101 55 (s, C(1, 1′)), 109.9 (s, C(6, 6′)), 111.3 (s, C(9, 9′)), 122.2 (s, C(10, 10′)), 122.8 (s, C(5, 5′)), 128.2 (s, C(3, 3′)), 140.6 (s, C(4, 4′)), 149.4 (s, C(7, 7′)), 151.2 (s, C(8, 8′)), 183.4 (s, C(2, 2′)═O).

2.1.1.2. HCurcII, (1E,4Z,6E)-5-hydroxy-1,7-bis(4-methoxyphenyl)hepta-1,4,6-trien-3-one.. To a solution of acetylacetone (11.2 mL, 0.1101 mol) in ethyl acetate (25 mL) was added anisaldehyde (25 g, 0.1836 mol), trimethyl borate (53.2 mL, 0.4774 mol) and *n*-butyl amine (2.7 mL, 0.0275 mol) at room temperature and the reaction mixture was heated to 65 °C and maintained at the same temperature for 6.0 h. After this period, the reaction mixture was cooled to room temperature and filtered. The reaction mass and the obtained residue were transferred into a

Please cite this article as: F. Caruso, et al., The in vitro antitumor activity of arene-ruthenium(II) curcuminoid complexes improves when decreasing curcumin polarity, J. Inorg. Biochem. (2016), http://dx.doi.org/10.1016/j.jinorgbio.2016.06.002

round bottom flask (0.5 L) and 10% acetic acid (250 mL) was added. The reaction mixture was stirred for 5 h at 110 °C. Then the reaction mass was cooled to room temperature, filtered and transferred into an round bottom flask (0.5 L); acetone (150 mL) was added and the temperature slowly raised to 65 °C. Afterwards water (150 mL) was added dropwise and the system refluxed for 2 h. Then the reaction mixture was cooled to room temperature and filtered. The obtained material was dried under vacuum for 2 h at 60 °C (13.5 g, 43.8% yield, HPLC purity: 99%). This is soluble in alcohols, acetone, acetonitrile, DMSO, chloro-hydrocarbon solvents. M.p.: 157–159 °C. Anal. Calcd. for $C_{21}H_{20}O_4$: C, 74.98: H, 5.99. Found: C, 74.22; H, 5.91; C, 74.69; H, 6.02. IR (cm^{-1}): 1509m ν(C═O), 1623m, 1601m, 1573m ν(C═C), 1176m ν(C—O). ^{1}H NMR ($CDCl_3$, 298 K): δ 3.85 (s, 6H, CH_3O), 5.78 (s, 1H, H—C1), 6.50 (d, 2H, ^3J = 16 Hz, H—C3, H—C3′), 6.91 (d, 4H, ^3J = 8 Hz, H—C7′, H—C9, H—C9′), 7.51 (d, 4H, ^3J = 8 Hz, H—C6, H—C6′, H—C10, H—C10′), 7.62 (d, 2H, ^3J = 16 Hz, H—C4, H—C4′), 16.00 (s, 1H, OH). ^{13}C {^{1}H} NMR ($CDCl_3$, 298 K): δ 55.6 (s, CH_3O), 101.6 (s, C1), 114.6 (s, C, C7′, C9, C9′), 122.0 (s, C3, C3′), 128.0 (s, C5, C5′), 130.0 (s, C6, C6′, C10, C10′), 140.3 (s, C4, C4′), 161.5 (s, C8, C8′), 183.6 (s, C═O).

2.1.2. Synthesis of ruthenium complexes

*2.1.2.1. [(η^6-p-cymene)Ru(CurcI)Cl] (**1**).* The ligand HCurcI (0.1998 g, 0.504 mmol) was dissolved in methanol (20 mL) and KOH (0.0282 g, 0.504 mmol) was added. The mixture was stirred for 1 h at room temperature, and then [Ru(η^6-*p*-cymene)Cl_2]$_2$ (0.1543 g, 0.252 mmol) was added. The resulting solution was refluxed and stirred 24 h. The solvent was removed under reduced pressure, and dichloromethane (10 mL) was added. The mixture was filtered to remove potassium chloride. The solution was concentrated to ca. 2 mL and stored at 4 °C. The red crystals obtained and collected (0.3150 g, 0.473 mmol, yield: 93%) were soluble in diethyl ether, alcohols, acetone, acetonitrile, DMSO, and chloro-hydrocarbon solvents. Anal. Calcd. for $C_{33}H_{37}ClO_6Ru$: C, 59.50; H, 5.60. Found: C, 59.10; H, 5.82. Λ_m ($(CH_3)_2SO$, 298 K, 10^{-3} mol L^{-1}): 3 S cm^{-2} mol^{-1}. IR (cm^{-1}): 1620m, 1598m, 1579m, 1500s ν(C═C, C═O). ^{1}H NMR ($CDCl_3$, 298 K): δ 1.39 (d, 6H, ^3J = 6.8 Hz, CH_3—C_6H_4—$CH(CH_3)_2$), 2.35 (s, 3H, CH_3—C_6H_4—$CH(CH_3)_2$), 3.00 (m, 1H, CH_3—C_6H_4—$CH(CH_3)_2$), 3.91 (s, 12H, CH_3O), 5.29 and 5.56 (4H, AA′BB′ system, CH_3—C_6H_4—$CH(CH_3)_2$ of *p*-cym, ^3J = 6 Hz), 5.48 (s, 1H, H—C1), 6.44 (d, 2H, ^3J = 16.0 Hz, H—C3, H—C3′), 6.85 (d, 2H, ^3J = 8.0 Hz, H—C9, H—C9′) 7.07 (s, 2H, H—C6, H—C6′), 7.10 (d, 2H, ^3J = 8.0 Hz, H—C10, H—C10′), 7.53 (d, 2H, ^3J = 16.0 Hz, H—C4, H—C4′). ^{13}C NMR ($CDCl_3$, 298 K): δ 18.3 (s, CH_3—C_6H_4—$CH(CH_3)_2$), 22.6 (s, CH_3—C_6H_4—$CH(CH_3)_2$), 31.0 (s, CH_3—C_6H_4—$CH(CH_3)_2$), 56.1 (s, CH_3O), 79.2, 83.2, 97.8, 99.7 (s, CH_3—C_6H_4—$CH(CH_3)_2$), 102.1 (s, C1), 109.7 (s, C6, C6′), 111.3 (s, C9, C9′), 122.2 (s, C10, C10′), 125.9 (s, C3, C3′), 129.1 (s, C5, C5′), 138.7 (s, C4, C4′), 149.3, 150.5 (s, C7, C7′, C8, C8′), 178.6 (s, C═O). ESI-MS (+) CH_3OH (*m/z*, relative intensity %): 631 [100] [(η^6-cym)Ru(CurcI)]$^+$. This compound has been reported [39] and its chemical characterization is consistent with our study. See also X-ray analysis below.

*2.1.2.2. [(η^6-benzene)Ru(CurcI)Cl] (**2**).* Compound **2** was prepared following a procedure similar to that reported for **1** by using [Ru(η^6-benzene)Cl_2]$_2$. **2** is soluble in alcohols, acetone, acetonitrile, DMSO and chloro-hydrocarbon solvents. Anal. Calcd. for $C_{29}H_{29}ClO_6Ru$: C, 57.09; H, 4.79. Found: C, 56.89; H, 4.82. Λ_m ($(CH_3)_2SO$, 298 K, 10^{-3} mol L^{-1}): 4 S cm^{-2} mol^{-1}. IR (cm^{-1}): 1619m, 1598m, 1580m, 1501s ν(C═C, C═O). ^{1}H NMR ($CDCl_3$, 298 K): δ 3.91 (s, 12H, —OCH_3), 5.52 (s, 1H, H—C1), 5.72, (s, 6H, H-benz), 6.47 (d, 2H, ^3J = 16 Hz, H—C3, H—C3′), 6.88 (d, 2H, ^3J = 8 Hz, H—C9, H—C9′) 7.08 (s, 2H, H—C6, H—C6′), 7.10 (d, 2H, ^3J = 8 Hz, H—C10, H—C10′), 7.58 (d, 2H, ^3J = 16 Hz, H—C4, H—C4′). ^{13}C {^{1}H} NMR ($CDCl_3$, 298 K): δ 56.1 (s, CH_3O), 82.7 (s, C_6H_6), 101.9 (s, C1), 109.9 (s, C6, C6′), 111.3 (s, C9, C9′), 122.1 (s, C10, C10′), 125.5 (s, C3, C3′), 129.0 (s, C5, C5′), 139.3 (s, C4, C4′), 149.3, 150.6 (s, C7, C7′, C8, C8′), 178.7 (s, C═O). ESI-MS (+) CH_3OH (*m/z*, relative intensity %): 575 [100] [(η^6-benz)Ru(CurcI)]$^+$.

*2.1.2.3. [(η^6-hexamethylbenzene)Ru(CurcI)Cl] = [(η^6-hmb)Ru(CurcI)Cl] (**3**).* It was prepared using a procedure similar to that reported for **1** by using [Ru(η^6-hmb)Cl_2]$_2$. **3** is soluble in alcohols, acetone, acetonitrile, DMSO and chloro-hydrocarbon solvents. Anal. Calcd. for $C_{35}H_{41}ClO_6Ru$: C, 60.55; H, 5.95. Found: C, 59.76; H, 5.89; C, 60.23; H, 6.04. Λ_m ($(CH_3)_2SO$, 298 K, 10^{-3} mol L^{-1}): 5 S cm^{-2} mol^{-1}. IR (cm^{-1}): 1500s ν(C═O), 1620m, 1598m, 1580m ν(C═C), 1139s ν(C—O). ^{1}H NMR ($CDCl_3$, 298 K): δ 2.13 (s, 18H, $C_6(CH_3)_6$), 3.92 (s, 12H, CH_3O), 5.42 (s, 1H, H—C1), 6.48 (d, 2H, ^3J = 16 Hz, H—C3, H—C3′), 6.85 (d, 2H, ^3J = 8 Hz, H—C9, H—C9′), 7.04 (s, 2H, H—C6, H—C6′), 7.09 (d, 2H, ^3J = 8 Hz, H—C10, H—C10′), 7.57 (d, 2H, ^3J = 16 Hz, H—C4, H—C4′). ^{13}C {^{1}H} NMR ($CDCl_3$, 298 K): δ 15.4 (s, $C_6(CH_3)_6$), 56.2 (s, CH_3O), 90.5 (s, $C_6(CH_3)_6$), 102.2 (C1), 109.8s (s, C6, C6′), 111.4 (s, C9, C9′), 122.0 (s, C10, C10′), 126.7 (s, C3, C3′), 129.3 (s, C5, C5′), 137.8 (s, C4, C4′), 149.4, 150.4 (s, C7, C7′, C8, C8′), 178.1 (s, C═O). ESI-MS (+) CH_3OH (*m/z*, relative intensity %): 659 [100] [(η^6-hmb)Ru(CurcI)]$^+$.

*2.1.2.4. [(η6-p-cymene)Ru(CurcII)Cl] (**4**).* Compound **4** was prepared following a procedure similar to that reported for **1** by using [Ru(η^6-*p*-cymene)Cl_2]$_2$ and HCurcII. **4** is soluble in alcohols, acetone, acetonitrile, DMSO and chloro-hydrocarbon solvents. Anal. Calcd. for $C_{31}H_{33}ClO_4Ru$: C, 61.43; H, 5.49. Found: C, 61.23; H, 5.36. Λ_m ($(CH_3)_2SO$, 298 K, 10^{-3} mol L^{-1}): 4 S cm^{-2} mol^{-1}. IR (cm^{-1}): 1502s ν(C═O), 1624m, 1601m, 1573m ν(C═C), 1168m ν(C—O). ^{1}H NMR ($CDCl_3$, 298 K): δ 1.39 (d, 6H, ^3J = 7.2 Hz, CH_3—C_6H_4—$CH(CH_3)_2$), 2.28 (s, 3H, CH_3—C_6H_4—$CH(CH_3)_2$), 2.98 (sep, 1H, ^3J = 6.8 Hz, CH_3—C_6H_4—$CH(CH_3)_2$), 3.83 (s, 6H, CH_3O), 5.43 (s, 1H, H—C1), 5.28, 5.55 (d, 4H, ^3J = 6 Hz, CH_3—C_6H_4—$CH(CH_3)_2$), 6.45 (d, 2H, ^3J = 16 Hz, H—C3, H—C3′), 6.88 (d, 4H, ^3J = 8 Hz, H—C7, H—C7′, H—C9, H—C9′), 7.46 (d, 4H, ^3J = 8 Hz, H—C6, H—C6′, H—C10, H—C10′), 7.56 (d, 2H, ^3J = 16 Hz, H—C4, H—C4′). ^{13}C {^{1}H} NMR ($CDCl_3$, 298 K): δ 18.2 (s, CH_3—C_6H_4—$CH(CH_3)_2$), 22.6 (s, CH_3—C_6H_4—$CH(CH_3)_2$), 31.1 (s, CH_3—C_6H_4—$CH(CH_3)_2$), 55.5 (s, CH_3O), 79.3, 83.2, 97.7, 99.7 (s, CH_3—C_6H_4—$CH(CH_3)_2$), 102.2 (s, C1), 114.4 (s, C7, C7′, C9, C9′), 125.7 (s, C3, C3′), 128.9 (s, C5, C5′), 129.5 (s, C6, C6′, C10, C10′), 138.5 (s, C4, C4′), 160.8 (s, C8, C8′), 178.6 (s, C═O). ESI-MS (+) CH_3OH (*m/z*, relative intensity %): 571 [100] [(η^6-cym)Ru(CurcII)]$^+$.

*2.1.2.5. [(η^6-benzene)Ru(CurcII)Cl] (**5**).* Compound **5** was prepared following a procedure similar to that reported for **1** by using [Ru(η^6-benzene)Cl_2]$_2$ and HCurcII. **5** is soluble in alcohols, acetone, acetonitrile, DMSO and chloro-hydrocarbon solvents. Anal. Calcd. for $C_{27}H_{25}ClO_4Ru$: C, 58.96; H, 4.58. Found: C, 58.84; H, 4.52. Λ_m ($(CH_3)_2SO$, 298 K, 10^{-3} mol L^{-1}): 5 S cm^{-2} mol^{-1}. IR (cm^{-1}): 1502m ν(C═O), 1622m, 1600m, 1572m ν(C═C), 1167s ν(C—O). ^{1}H NMR ($CDCl_3$, 298 K): δ 3.79 (s, 6H, CH_3O), 5.43 (s, 1H, H—C1), 5.68 (s, 6H, C_6H_6), 6,42 (d, 2H, ^3J = 16 Hz, H—C3, H—C3′), 6.85 (d, 4H, ^3J = 8 Hz, H—C7, H—C7′, H—C9, H—C9′), 7.44 (d, 4H, ^3J = 8 Hz, H—C6, H—C6′, H—C10, H—C10′), 7.56 (d, 2H, ^3J = 16 Hz, H—C4, H—C4′). ^{13}C {^{1}H} NMR ($CDCl_3$, 298 K): δ 55.6 (s, CH_3O), 82.7 (s, C_6H_6), 102.1 (s, C1), 114.5 (s, C7, C7′, C9, C9′), 125.2 (s, C3, C3′), 128.7 (s, C5, C5′), 129.6 (s, C6, C6′, C10, C10′), 139.1 (s, C4, C4′), 160.9 (s, C8, C8′), 178.7 (s, C═O). ESI-MS (+) CH_3OH (*m/z*, relative intensity %): 515 [100] [(η^6-benz)Ru(CurcII)]$^+$.

*2.1.2.6. [(η^6-hmb)Ru(CurcII)Cl] (**6**).* Compound **6** was prepared following a procedure similar to that reported for **1** by using [Ru(η^6-hmb)Cl_2]$_2$ and HCurcII. **6** is soluble in alcohols, acetone, acetonitrile, DMSO and chloro-hydrocarbon solvents. Anal. Calcd. for $C_{33}H_{37}ClO_4Ru$: C, 62.50; H, 5.88. Found: C, 62.29; H, 5.71. Λ_m ($(CH_3)_2SO$, 298 K, 10^{-3} mol L^{-1}): 5 S cm^{-2} mol^{-1}. IR (cm^{-1}): 1502m ν(C═O), 1625m, 1601m, 1575m, 1532m ν(C═C), 1159s ν(C—O). ^{1}H NMR ($CDCl_3$, 298 K): δ 2.12 (s, 18H, $C_6(CH_3)_6$), 3.83 (s, 6H, CH_3O), 5.37 (s, 1H, H—C1), 6.48 (d, 2H,

^3J = 16 Hz, H—C3, H—C3′), 6.88 (d, 4H, ^3J = 8 Hz, H—C7, H—C7′, H—C9, H—C9′), 7.46 (d, 4H, ^3J = 8 Hz, H—C6, H—C6′, H—C10, H—C10′), 7.59 (d, 2H, ^3J = 16 Hz, H—C4, H—C4′). ^{13}C {^{1}H} NMR ($CDCl_3$, 298 K): δ 15.4 (s, $C_6(CH_3)_6$), 55.6 (s, CH_3O), 90.5 (s, $C_6(CH_3)_6$), 102.4 (s, C1), 114.4 (s, C7, C7′, C9, C9′), 126.4 (s, C3, C3′), 129.0 (s, C5, C5′), 129.4 (s, C6, C6′, C10, C10′), 137.6 (s, C4, C4′), 160 (s, C8, C8′), 178.1 (s, C═O). ESI-MS (+) CH_3OH (*m/z*, relative intensity %): 599 [100] [(η^6-hmb)Ru(CurcII)]$^+$.

2.1.3. X-ray study of HCurcI

Suitable crystals for X-ray diffraction data collection were obtained by dissolving a sample in a mixture of 1:1 methanol/*n*-hexane solution and left standing at room temperature for a week. Using a needle crystal 1464 frames were collected on a Bruker Apex II diffractometer at 125 K. The total exposure time was 18.30 h. The frames were integrated with the Bruker SAINT software package using a narrow-frame algorithm. Data were corrected for absorption effects using the multi-scan method SADABS. The structure was solved and refined using the Bruker SHELXTL Software Package [40]. Table 1 shows crystallographic and refinement data. CCDC 1040262 contains the supplementary crystallographic data for this paper that can be obtained free of charge from The Cambridge Crystallographic Data Centre via www.ccdc.cam.ac.uk/data_request/cif. Complex [(η^6-*p*-cymene)Ru(CurcI)Cl] was also studied with diffraction methods. The cell parameters were the same as those reported in the literature [39], confirming its molecular structure.

2.1.4. Cell lines and in vitro culture conditions

The cell lines MCF7 (HTB-22, human breast adenocarcinoma), HCT116 (CCL-247, human colorectal carcinoma), A549 (CCL-185, human lung carcinoma) and U-87 MG (HTB-1, human glioblastoma) were obtained from ATCC (American Type Culture Collection, Manassas, VA, USA); A2780 human ovarian carcinoma were obtained from ECACC (European Collection of Animal Cell Culture, Salisbury, U.K.). They were maintained under standard culture conditions (37 °C; 5% CO_2) in DMEM medium (Euroclone, Milan, Italy), supplemented with 10% fetal calf serum (Euroclone, Milan, Italy), 1% glutamine and 1% antibiotics mixture; for HCT116 and U-87 MG cells 1% sodium pyruvate and 1% non-essential amino acids (both from Sigma-Aldrich, Milan, Italy) were also added to the culture medium. All experiments were performed within 10 passages from thawing.

Table 1
Crystal data and structure refinement for HCurcI, (1E,4Z,6E)-5-hydroxy-1,7-bis(3,4-dimethoxyphenyl)hepta-1,4,6-trien-3-one.

Empirical formula	$C_{23}H_{24}O_6$
Formula weight	396.42
Temperature	125(2) K
Wavelength	0.71073 Å
Crystal system	Monoclinic
Space group	$P2_1/n$
Unit cell dimensions	a = 7.8984(5) Å b = 26.9720(16) Å c = 18.8836(11) Å β = 100.846(1)°
Volume	3951.0(4) Å^3
Z	8
Density (calculated)	1.333 Mg/m^3
Absorption coefficient	0.096 mm^{-1}
F(000)	1680
Crystal size	0.28 × 0.09 × 0.05 mm^3
Crystal color, shape	Pale yellow, needle
2-Theta range for data collection	4.64° < 2θ < 55.0°
Index ranges	−10 ≤ h ≤ 10, −35 ≤ k ≤ 35, −24 ≤ l ≤ 24
Reflections collected	52,703
Independent reflections	9260
Completeness to theta = 27.50°	100%
Absorption correction	Empirical
Max. and min. transmission	0.995 and 0.974
Refinement method	Full-matrix least-squares on F^2
Data/restraints/parameters	7162/0/715
Goodness-of-fit on F^2	1.213
Final R indices [I > 2sigma(I)]	*R*1 = 0.0523, w*R*2 = 0.0569
R indices (all data)	*R*1 = 0.0666, w*R*2 = 0.1344
Largest diff. peak and hole	−0.261 and 0.051 e·Å^{-3}

2.1.4.1. Ru complexes administered.

The four compounds under study were reconstituted in sterile DMSO at a concentration of 1 M; stock solutions were then diluted to the desired final concentrations with sterile complete medium immediately before each experiment. The final DMSO concentration never exceeded 0.2%, which was not toxic to the cells under the drug exposure conditions used in this study. Curcumin, HCurcI and HCurcII were also analyzed following the same protocol.

2.1.4.2. Growth inhibition assay.

The 3-(4,5-dimethylthiazol-2-yl)-2,5-diphenyltetrazolium bromide (MTT) assay was performed on all the cell lines tested as described [41] with minor modifications. Briefly, according to the growth profiles previously defined for each cell line, adequate numbers of cells were plated in each well of a 96-well plate in 0.1 mL of complete culture medium and allowed to attach for 24 h. Cells were exposed at 37 °C for 72 h to the four compounds at concentrations ranging between 5 and 750 μM, bringing the final volume to 0.2 mL/well. Each experiment included 8 replications per concentration tested; control samples were run with 0.2% DMSO. At the end of the period of incubation, MTT (0.05 mL of a 2 mg/mL stock solution in PBS) was added to each well for 3 h at 37 °C. Cell supernatants were then carefully removed, the blue formazan crystals formed through MTT reduction by metabolically active cells were dissolved in 0.120 mL DMSO and the corresponding optical densities were measured at 570 nm, using a Universal Microplate Reader EL800 (Bio-TekWinooski, VT). IC_{50} values were estimated from the resulting concentration-response curves by non-linear regression analysis, using GraphPad Prism software, v. 5.0 (GraphPad, San Diego, CA, USA). Differences between IC_{50} values were evaluated statistically by analysis of variance with Bonferroni post-test for multiple comparisons. Cell cycle effects, as well as the ability to induce apoptosis and generation of reactive oxygen species (ROS), were assessed for representative compounds on representative cell lines as follows.

2.1.4.3. Cell cycle analysis and percentage of apoptotic cells.

Following 72 h-exposure to HCurcI and [(η^6-*p*-cymene) Ru(CurcI)Cl], 5 × 10^5 cells were fixed in 0.5 mL of ice-cold 100% ethanol and stored at −20 °C. Cells were then centrifuged, washed with PBS, resuspended in the dying solution (50 μg/mL propidium iodide, 20 μg/mL RNase in 1× PBS) and analyzed with FACScalibur flow cytometer (Becton–Dickinson, Mountain View, CA, USA) equipped with a 15-mW, 488-nm, air-cooled argon ion laser. Fluorescent emissions were collected through a 530-nm band-pass filter for fluorescein, a 575-nm band-pass filter for PI. At least 10,000 events were analyzed for each sample. Data were processed using CellQuest software (Becton-Dickinson). The percentage of apoptotic cells in each sample was determined based on the sub-G1 peaks detected in monoparametric histograms.

2.1.4.4. Detection of reactive oxygen species.

Induction of intracellular ROS generation by HCurcI and [(η^6-*p*-cymene) Ru(CurcI)Cl] peroxides was assessed by flow cytometric analysis of the cells following 72 h-exposure to the two compounds using 2,7-Dichlorodihydrofluorescein diacetate (10 μM for 45 min in the dark at 37 °C) as a fluorogenic probe.

2.1.5. Computational study

The theoretical study involved calculations using software programs from Biovia-Accelrys [42]. Density functional theory code DMol3 was used to calculate energy, geometry and frequencies implemented in Materials Studio 5.5 (PC platform) [43]. We employed the double numerical polarized (DNP) basis set that includes all the occupied atomic orbitals plus a second set of valence atomic orbitals, and polarized d-

Please cite this article as: F. Caruso, et al., The in vitro antitumor activity of arene-ruthenium(II) curcuminoid complexes improves when decreasing curcumin polarity, J. Inorg. Biochem. (2016), http://dx.doi.org/10.1016/j.jinorgbio.2016.06.002

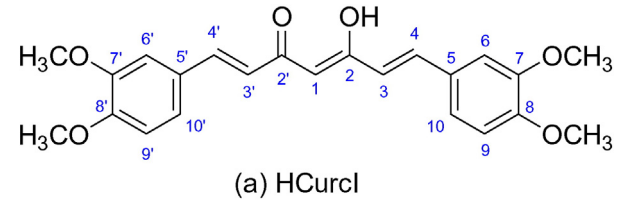

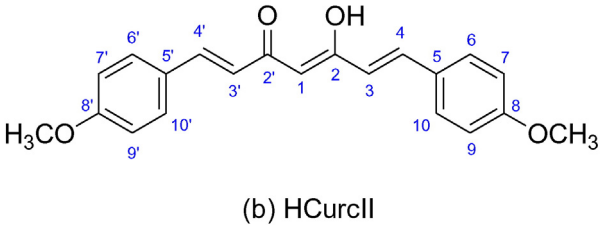

Scheme 1. HCurcI and HCurcII ligands.

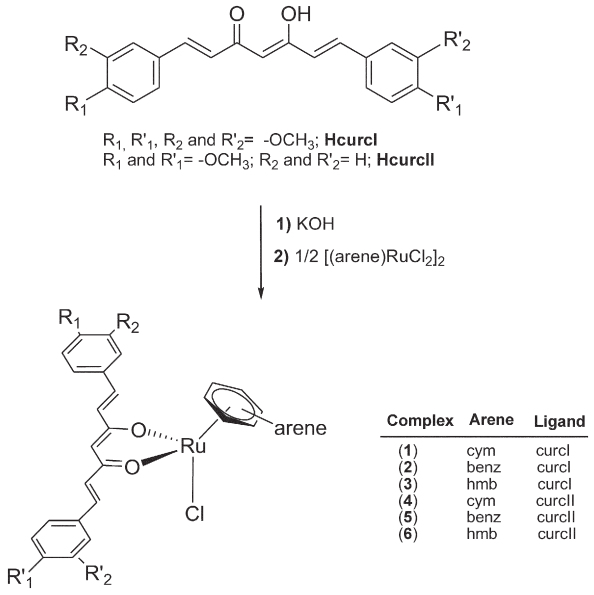

Scheme 2. Ru complex synthesis.

valence orbitals [44], and correlation generalized gradient approximation (GGA) was applied in the manner suggested by Perdew-Burke-Ernzerhof (PBE) [45], including all electrons explicitly. The real space cutoff of 5 Å was imposed for numerical integration of the Hamiltonian matrix elements. The self-consistent-field convergence criterion was set to the root-mean-square change in the electronic density to be less than 10^{-6} electrons/Å^3. The convergence criteria applied during geometry optimization were $2.72 \cdot 10^{-4}$ eV for energy and 0.054 eV/Å for force. Calculations of AlogP [46] were done using Discovery Studio version 4.1, after geometry optimization of curcumin, HCurcI and HCurcII and verification of their converged structures representing minimums.

3. Results and discussion

Ru^{II}-arene complexes **1**–**6** were prepared in high yield from the reaction of the appropriate dimer, $[Ru(\eta^6\text{-arene})Cl_2]_2$ with the corresponding curcumin related ligand and KOH in methanol (Scheme 2).

The complexes are air-stable in solution and in the solid-state and are highly soluble in most organic solvents. The IR spectra of **1**–**6** show the typical shift of the ν(C═O) vibrations to lower frequency upon ligand coordination to the metal ion. In the positive ESI mass

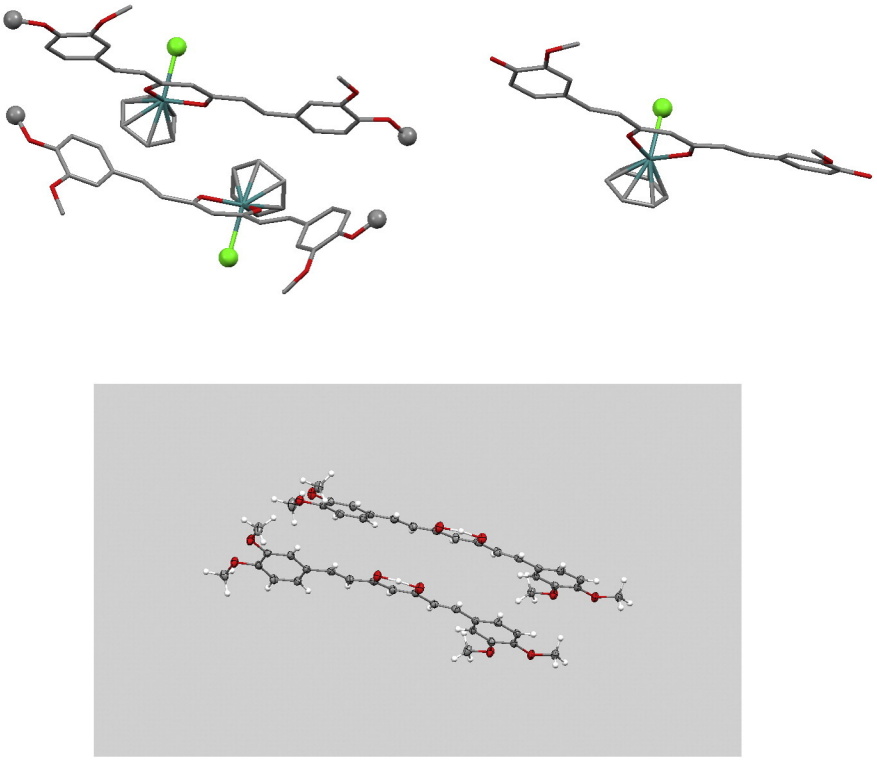

Fig. 1. Display of the two molecules in asymmetric unit of compound **1** (top left) and [(η^6-*p*-cymene)Ru(Curc)Cl] (top right). The top molecule of compound **1** and [(η^6-*p*-cymene)Ru(Curc)Cl] have similar planar conformations. H atoms and the methyl and isopropyl groups on cymene are omitted for clarity. Atoms in top molecules are in stick style, except for the only chemical difference between both compounds: the methyl group in *para* position in **1** instead of OH in [(η^6-*p*-cymene)Ru(Curc)Cl] (ball style); also Cl atoms are ball style. In the X-ray structure of HCurcI, ellipsoids 50% (bottom), the 2 molecules have slight differences and similar planar conformation.

Please cite this article as: F. Caruso, et al., The in vitro antitumor activity of arene-ruthenium(II) curcuminoid complexes improves when decreasing curcumin polarity, J. Inorg. Biochem. (2016), http://dx.doi.org/10.1016/j.jinorgbio.2016.06.002

Table 2
Antiproliferative effect of Ru complexes (**1**–**4**) on five human cancer cell lines. IC_{50} values (μM) are the mean values ± SE of 3–5 independent experiments and were extrapolated from dose response curves obtained at the end of 72-h incubation in the presence of the compounds. The highest biological activity for each cell line is indicated in bold. Note: hmb = hexamethylbenzene. [(η^6-*p*-cymene)Ru(Curc)Cl] [27] is also included for comparison.

Cell line/compound		A2780	A549	MCF7	HCT116	U87
HCurcI		1.5 ± 0.3[i]	3.7 ± 0.5[k,j]	1.76 ± 0.16[i]	1.83 ± 0.20[i]	9.3 ± 2.0[i]
HCurcII		43.8 ± 1.9[k]	53.2 ± 1.9[k]	29.7 ± 6.8[k]	24.2 ± 6.5[j]	41.5 ± 9.7[k]
Curcumin		4.3 ± 1.7	14.7 ± 1.8	10.5 ± 2.6	5.8 ± 0.8	12.7 ± 2.1
[(η^6-*p*-Cymene) Ru(CurcI)Cl]	**1**	**9.4** ± 1.0[c,d,f]	**13.7** ± 0.6[b,e,g,i]	10.6 ± 1.6[a,i]	**15.5 ± 2.7**	**9.4** ± 0.7[i]
[(η^6-Benzene) Ru(CurcI)Cl]	**2**	28.3 ± 2.3[g,i,k]	20.6 ± 0.7[a,g,i]	11.6 ± 1.8[a,i]	19.2 ± 0.5	21.4 ± 2.8[h]
[(η^6-hmb) Ru(CurcI)Cl]	**3**	11.4 ± 0.8[c,d,g,i]	15.5 ± 1.7[b,e,g,i]	**9.7** ± 0.3[b,i]	32.6 ± 5.7[g,k]	10.9 ± 0.6[i]
[(η^6-Cymene) Ru(CurcII)Cl]	**4**	21.2 ± 2.1[g,i,k]	30.6 ± 1.1[g,i]	25.2 ± 2.3[g,k]	15.9 ± 3.1	21.2 ± 4.3[h]
[(η^6-*p*-Cymene) Ru(Curc)Cl]		23.4 ± 3.3	63.2 ± 8.9	19.6 ± 2.4	**14.0** ± 1.5	62.3 ± 8.9

[a] $p < 0.01$ vs **4**.
[b] $p < 0.001$ vs **4**.
[c] $p < 0.01$ vs **2**.
[d] $p < 0.05$ vs **4**.
[e] $p < 0.05$ vs **2**.
[f] $p < 0.05$ vs HCurcI.
[g] $p < 0.01$ vs HCurcI.
[h] $p < 0.05$ vs HCurcII.
[i] $p < 0.01$ vs HCurcII.
[j] $p < 0.05$ vs curcumin.
[k] $p < 0.01$ vs curcumin.

spectra of **1**–**6** species peaks due to the cationic fragments [Ru(η^6-arene)(CurcI)]$^+$ and [Ru(η^6-arene)(CurcII)]$^+$, are observed as the predominant species; they are generated from loss of Cl^-. The ^1H spectra of **1**–**6** display a distinct shift of resonances of the ligand protons in comparison with their equivalents in the free ligands.

In the X-ray structure of HCurcI, the keto-enol arrangement (scheme 1) is preferred to the diketo form. This configuration is the same found experimentally in curcumin X-ray structure [47], and calculated theoretically [48]. A comparison between the already solved crystal structures of [(η^6-*p*-cymene)Ru(Curc)Cl] [36] and compound **1** [39] shows that in the former there is a single molecule in the asymmetric unit showing the curcumin ligand (Fig. 1 top right) twisted at the aromatic rings. Compound **1**, [(η^6-*p*-cymene)Ru(CurcI)Cl], has two molecules in the asymmetric unit that are markedly different: one is a molecule similar to [(η^6-*p*-cymene)Ru(Curc)Cl], whereas the other is significantly arched (Fig. 1, top-left, bottom molecule). The ligand HCurcI (Fig. 1, bottom) also contains two molecules in the asymmetric unit and both display similarity with the basic curcumin ligand as it appears in [(η^6-*p*-cymene)Ru(Curc)Cl]. Since curcumin deformation may influence its interaction with DNA, we performed DFT calculations to verify energetically how much the arched conformation differs from the other one in the same asymmetric unit of compound **1**. To do these calculations the Cl, *p*-cymene and Ru atom were eliminated from the (*p*-cymene)Ru-(CurcI)Cl containing the arched conformation, H was added to regenerate the keto-enol fragment and a geometrical optimization was performed and a restraint on all CurcI torsion angles was imposed. The corresponding energy minimum was verified (it showed no imaginary frequencies) and compared with that obtained from the geometry optimization of HCurcI X-ray coordinates with no imposed restriction. The latter conformation has lower energy by 3.3 kcal/mol. The arched conformation in the crystal is due to a π-π interaction between its *p*-cymene and an aromatic ring of the other molecule; we are executing further studies to clarify this point [49], since DNA interaction with curcumin is mainly determined by its peripheral functional groups, i.e. the keto-enol moiety does not participate directly to the binding [36]. The arched conformation, found in the X-ray structure, gives a potential indication of how the curcuminoid ligands could be accommodated when interacting with DNA, but it is not evidence of its existence.

The antitumor activity of 4 complexes and curcuminoids was studied in vitro on 5 cell lines and is shown in Table 2, which also includes the previously obtained data for the parent compound [(η^6-*p*-cymene)Ru(Curc)Cl] [29]. It is generally observed that substitution of two OH groups in curcumin by (a) OCH_3 groups to form HCurcI, or (b) H to give HCurcII, induces higher antitumor activity in their complexes than observed for the parent curcumin complex [(η^6-*p*-cymene)Ru(Curc)Cl]. Thus, in the MCF7 breast cell line the activity (IC_{50}) of [(η^6-hexamethylbenzene)Ru(CurcI)Cl] is double that of the curcumin complex, 9.7 vs 19.6 μM, respectively; in the A2780 ovarian cell line activity of [(η^6-*p*-cymene)Ru(CurcI)Cl] is improved by a 2.4 factor (23.4/9.4); in the A549 lung cancer cell line [(η^6-*p*-cymene)Ru(CurcI)Cl] is 4.6 times more active (63.2/13.7) whereas in the U87 glioblastoma cell line it is 6.6 times stronger (62.3/9.4). Only in the HCT116 colon cell line do our novel complexes show no improvement, [(η^6-*p*-cymene)Ru(Curc)Cl] (IC_{50} = 14.0 μM). In fact, [(η^6-cymene)Ru(CurcI)Cl] (15.5 μM) and [(η^6-cymene)Ru(CurcII)Cl] (15.9 μM) have similar activity. On the whole it seems that substitution on the curcumin skeleton plays a very important role in activity, perhaps more than that of Ru complexation, except in the case of CurcII ligand, where the influence of the metal is, instead, more important. Biological studies performed in A2780, MCF7 and U87 cells indicate

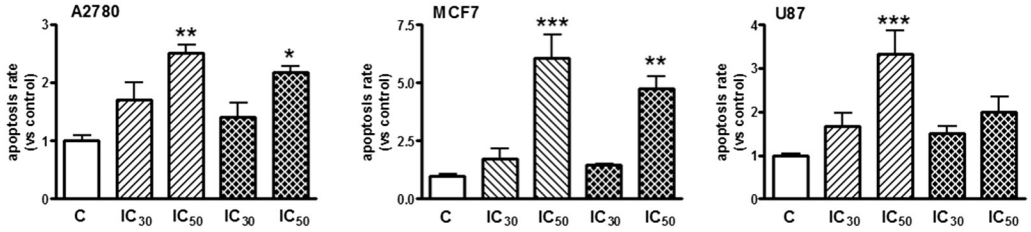

Fig. 2. Apoptotic effects of HCurcI (hatched bars) and [(η^6-*p*-cymene) Ru(CurcI)Cl] (cross-hatched bars) on A2780, MCF7 and U87 cells. Cells were exposed for 72 h to concentrations of the two compounds corresponding to their respective IC_{30} and IC_{50} values in the cell lines. The percentage of apoptotic cells was assessed by flow cytometry analysis of propidium iodide-stained cells and normalized versus untreated cell samples (C). Values are the mean ± SEM of 3–4 independent experiments. *$p < 0.05$ vs C; **$p < 0.01$ vs C; ***$p < 0.001$ vs C.

Please cite this article as: F. Caruso, et al., The in vitro antitumor activity of arene-ruthenium(II) curcuminoid complexes improves when decreasing curcumin polarity, J. Inorg. Biochem. (2016), http://dx.doi.org/10.1016/j.jinorgbio.2016.06.002

that HCurcI and [(η^6-*p*-cymene)Ru(CurcI)Cl] induce concentration-dependent apoptotic cell death (Fig. 2) in all three cell lines, without perturbing cell cycle progression (Supplementary Fig. S1).

Related cell studies on a series of dinuclear arene ruthenium complexes (η^6-*p*-cymene)RuCl(*O-O′-R-O-O′*)RuCl(η^6-*p*-cymene), where R contains a —$(CH_2)_n$— spacer, and having the same keto-enol coordination sphere, correlate antitumor activity with increasing ligand lipophilicity [50]. This resembles our study, where lack of curcumin hydroxyl substituents in HCurcI and HCurcII leads to higher lipophilicity compared to, as shown by our calculated AlogP of 2.182, 2.612 and 1.36, respectively.

Among curcuminoids HCurcII has the lowest activity, Table 2, but, in A2780, A549 and U87 cell lines, [(η^6-cymene)Ru(CurcII)Cl] has improved cytotoxicity by a factor of about 2.

As shown in this study, the Ru-arene complexes with less polar and more lipophilic curcumin-derivative ligands are biologically more effective than [(η^6-*p*-cymene)Ru(Curc)Cl]. However, the antioxidant features of curcumin should be considered. In general, the antioxidant property of polyphenols, a class of compounds that includes curcumin, is directly related to the number of hydroxyls bound to their aromatic rings [51].

The ligands in the title compounds contain no hydroxyl groups, causing ligand antioxidant features to differ markedly from the parent curcumin. In fact, the antioxidant features, associated with many important biological processes, would be non-existent in the present Ru complexes. Therefore, in this study, in addition to the biological activity of novel Ru-arene-curcuminoids correlated to less polarity and greater lipophilicity, a potential correlation between cytotoxicity and the decreased antioxidant features in the Ru ligands was investigated. We explored ROS production in our system and found that this was only detected marginally in U87 cells (Supplementary Fig. S2) upon treatment with the two compounds which show apoptotic features, HCurcI and [(η^6-*p*-cymene)Ru(CurcI)Cl]. We conclude that ROS production is unlikely to contribute significantly to the observed cytotoxicity.

Hydrolysis of Ru^{II}-arene antitumor compounds is considered a central feature for their activity. For example, the biphenyl species [(Ph-Ph)Ru(ethylenediamine)Cl]$^+$ has a hydrolysis reaction about 20 times faster than that of cisplatin, and its binding is reversible upon addition of [NaCl] equivalent to blood plasma [52]. It is generally accepted that Ru—Cl hydrolysis is important for Ru interaction with N7-guanine DNA. In this study we show that Ru(arene)(L)Cl complexes, L = Curc and CurcI, do not improve Curc and CurcI in vitro antiproliferative activity. However, such improvement could be feasible, if Cl is replaced by the neutral ligand PTA (1,3,5-triaza-7-phosphaadamantane). This ligand substitution was recently reported for the activity in the cisplatin resistant cell line A2780 (IC_{50} = 0.36 μM) [53], and was higher than in the parent compound [(η^6-*p*-cymene)Ru(Curc)Cl] (25 μM). In addition, a recent study showed that when chlorido is replaced by iodido in arene-Ru^{II} complexes a surprising greater biological activity is found [54]. Therefore, an adequate replacement of chloride leaving group in the coordination sphere of Ru-(arene) curcuminoids by anionic or neutral species, may improve curcuminoid antitumor activity. Further investigation on Ru(arene) curcuminoids is therefore warranted and may help to clarify if Ru—Cl bond hydrolysis is as important to complex activity as Cl^- hydrolysis in cisplatin. In summary, the results of our study show that, with only one exception, the CurcII ligand, chemical substitution on the curcumin skeleton seems to produce biologically more efficient molecules, as shown by lower IC_{50}, than does their complexation to arene-ruthenium^{II} species. Biological tests on other Ru complexes may clarify these findings.

Abbreviations

HCurcI	(1E,4Z,6E)-5-hydroxy-1,7-bis(3,4-dimethoxyphenyl)hepta-1,4,6-trien-3-one
HCurcII	(1E,4Z,6E)-5-hydroxy-1,7-bis(4-methoxyphenyl)hepta-1,4,6-trien-3-one)

Supplementary data to this article can be found online at http://dx.doi.org/10.1016/j.jinorgbio.2016.06.002.

Acknowledgements

Vassar College Research Committee.

References

[1] L. Ronconi, P.J. Sadler, Coord. Chem. Rev. 251 (2007) 1633–1648.
[2] P.J. Dyson, Chimia 61 (2007) 698–703.
[3] I. Bratsos, S. Jedner, T. Gianferrara, E. Alessio, Chimia 61 (2007) 692–697.
[4] C.G. Hartinger, M.A. Jakupec, S. Zorbas-Seifried, B. Kynast, H. Zorbas, B.K. Keppler, Chem. Biodivers. 5 (2008) 2140–2155.
[5] M.A. Jakupec, M. Galanski, V.B. Arion, C.G. Hartinger, B.K. Keppler, Dalton Trans. (2008) 183–194.
[6] Y.K. Yan, M. Melchart, A. Habtemariam, P.J. Sadler, Chem. Commun. (2005) 4764–4776.
[7] J. Reedijk, Platin. Met. Rev. 52 (2008) 2–11.
[8] S.M. Guichard, R. Else, E. Reid, B. Zeitlin, R. Aird, M. Muir, M. Dodds, H. Fiebig, P.J. Sadler, D.I. Jodrell, Biochem. Pharmacol. 71 (2006) 408–415.
[9] R.E. Aird, R.J. Cummings, A.A. Ritchie, M. Muir, R.E. Morris, H. Chen, P.J. Sadler, D.I. Jodrell, Brit. J. Cancer 86 (2002) 1652–1657.
[10] O. Novakova, H. Chen, O. Vrana, A. Rodger, P.J. Sadler, V. Brabec, Biochemistry 42 (2003) 11544–11554.
[11] C.G. Hartinger, P.J. Dyson, Chem. Soc. Rev. 38 (2009) 391–401.
[12] M. Melchart, P.J. Sadler, in: G. Jaouen (Ed.), Bioorganometallics, Wiley-VCH, Weinheim 2006, pp. 39–63.
[13] G. Suss-Fink, Dalton Trans. 39 (2010) 1673–1688.
[14] A.A. Nazarov, C.G. Hartinger, P.J. Dyson, J. Organomet. Chem. 751 (2014) 251–260.
[15] G. Suss-Fink, J. Organomet. Chem. 751 (2014) 2–19.
[16] R.E. Morris, R.E. Aird, P.d.S. Murdoch, H. Chen, J. Cummings, N.D. Hughes, S. Pearsons, A. Parkin, G. Boyd, D.I. Jodrell, P.J. Sadler, J. Med. Chem. 44 (2001) 3616–3621.
[17] H.-K. Liu, F. Wang, J.A. Parkinson, J. Bella, P.J. Sadler, Chem. Eur. J. 12 (2006) 6151–6165.
[18] O. Novakova, H. Chen, O. Vrana, A. Rodger, P.J. Sadler, V. Brabec, Biochemistry 42 (2003) 11544–11554.
[19] F. Wang, H. Chen, J.A. Parkinson, P.d.S. Murdoch, P.J. Sadler, Inorg. Chem. 41 (2002) 4509–4523.
[20] H. Petzold, J. Xu, P.J. Sadler, Angew. Chem. Int. Ed. 47 (2008) 3008–3011.
[21] S.J. Dougan, P.J. Sadler, Chimia 61 (2007) 704–715.
[22] H. Chen, J.A. Parkinson, S. Parsons, R.A. Coxall, R.O. Gould, P.J. Sadler, J. Am. Chem. Soc. 124 (2002) 3064–3082.
[23] F. Caruso, E. Monti, J. Matthews, M. Rossi, M.B. Gariboldi, C. Pettinari, R. Pettinari, F. Marchetti, Inorg. Chem. 53 (2014) 3668–3677.
[24] W.S. Sheldrick, S. Heeb, Inorg. Chim. Acta 168 (1990) 93–100.
[25] F. Pelletier, V. Comte, A. Massard, M. Wenzel, S. Toulot, P. Richard, M. Picquet, P. Le Gendre, O. Zava, F. Edafe, A. Casini, P.J. Dyson, J. Med. Chem. 53 (2010) 6923–6933.
[26] A. Casini, C. Gabbiani, F. Sorrentino, M.P. Rigobello, A. Bindoli, T.J. Geldbach, A. Marrone, N. Re, C.G. Hartinger, P.J. Dyson, L. Messori, J. Med. Chem. 51 (2008) 6773–6781.
[27] P. Nowak-Sliwinska, J.R. van Beijnum, A. Casini, A.A. Nazarov, G. Wagnieres, H. van den Bergh, P.J. Dyson, A.W. Griffioen, J. Med. Chem. 54 (2011) 3895–3902.
[28] M. Groessl, M. Terenghi, A. Casini, L. Elviri, R. Lobinski, P.J. Dyson, J. Anal. At. Spectrom. 25 (2010) 305–313.
[29] C.G. Hartinger, A. Casini, C. Duhot, Y.O. Tsybin, L. Messori, P.J. Dyson, J. Inorg. Biochem. 102 (2008) 2136–2141.
[30] G.E. Atilla-Gokcumen, L. Di Costanzo, E. Meggers, J. Biol, Inorg. Chem. 16 (2011) 45–50.
[31] Z. Adhireksan, G.E. Davey, P. Campomanes, M. Groessl, C.M. Clavel, H. Yu, A.A. Nazarov, C.H.F. Yeo, W.H. Ang, P. Droge, U. Rothlisberger, P.J. Dyson, C.A. Davey, Nat. Commun. 5 (2014) 1–13.
[32] P.J. Dyson, G. Sava, Dalton Trans. (2006) 1929–1933.
[33] W. Guo, W. Zheng, Q. Luo, X. Li, Y. Zhao, S. Xiong, F. Wang, Inorg. Chem. 52 (2013) 5328–5338.
[34] F. Caruso, M. Rossi, A. Benson, C. Opazo, D. Freedman, E. Monti, M.B. Gariboldi, J. Shaulky, F. Marchetti, R. Pettinari, C. Pettinari, J. Med. Chem. 55 (2012) 1072–1081.
[35] R.K. Maheshwari, A.K. Singh, J. Gaddipati, R.C. Srimal, Life Sci. 27 (2006) 2081–2087.
[36] B.B. Aggarwal, C. Sundaram, N. Malani, H. Ichikawa, Adv. Exp. Med. Biol. 595 (2007) 1–75.
[37] A.F. Peacock, A. Habtemariam, R. Fernández, V. Walland, F.P. Fabbiani, S. Parsons, R.E. Aird, D.I. Jodrell, P.J. Sadler, J. Amer. Chem. Soc. 128 (2006) 1739–1748.
[38] X. Lei, W. Su, P. Li, Q. Xiao, S. Huang, Q. Qian, C. Huang, D. Qin, H. Lan, Polyhedron 81 (2014) 614–618.
[39] F. Kuhlwein, K. Polborn, W. Beck, Z. Anorg. Allg. Chem. 623 (1997) 1211–1219.
[40] G.M. Sheldrick, SHELXTL, An Integrated System for Solving, Refining and Displaying Crystal Structures From Diffraction Data, University of Gottingen, Gottingen, Germany, 1981.
[41] D.A. Scudiero, R.H. Shoemaker, K.D. Paull, A. Monks, S. Tierney, T.H. Nofziger, M.J. Currens, D. Seniff, M.R. Boyd, Cancer Res. 48 (1988) 4827–4833.
[42] Accelrys, Inc. 10188 Telesis Court, Suite 100, San Diego, CA 92121, USA.
[43] B. Delley, J. Chem. Phys. 113 (2000) 7756–7764.

[44] J.P. Perdew, J.A. Chevary, S.H. Vosko, K.A. Jackson, M.R. Pederson, D.J. Singh, C. Fiolhais, Phys. Rev. B: Cond. Mat. Mater. Phys. 46 (1992) 6671–6687.
[45] A.D. Becke, Phys. Rev. A 38 (1988) 3098–3100.
[46] A.K. Ghose, G.M. Crippen, J. Comput. Chem. 7 (1986) 565–577.
[47] P. Sanphui, N.R. Goud, U.B.R. Khandavilli, S. Bhanoth, A. Nangia, Chem. Commun. 47 (2011) 5013–5015.
[48] F. Caruso, C. Pettinari, F. Marchetti, M. Rossi, C. Opazo, S. Kumar, S. Balwani, B. Ghosh, Bioorg. Med. Chem. 17 (2009) 6166–6172.
[49] Caruso, F. et al. (Manuscript in preparation).
[50] M.G. Mendoza-Ferri, C.G. Hartinger, M.A. Mendoza, M. Groessl, A.E. Egger, R.E. Eichinger, J.B. Mangrum, N.P. Farrell, M. Maruszak, P.J. Bednarski, F. Klein, M.A. Jakupec, A.A. Nazarov, K. Severin, B.K. Keppler, J. Med. Chem. 52 (2009) 916–925.
[51] M. Rossi, F. Caruso, C. Opazo, J. Salciccioli, J. Agric, Food Chem. 56 (2008) 10557–10566.
[52] F. Wang, H. Chen, S. Parsons, I.D.H. Oswald, J.E. Davidson, P.J. Sadler, Chem. Eur. J. 9 (2003) 5810–5820.
[53] R. Pettinari, C. Pettinari, F. Marchetti, C.M. Clavel, R. Scopelliti, P.J. Dyson, Organometallics 32 (2013) 309–316.
[54] I. Romero-Canelón, L. Salassa, P.J. Sadler, J. Med. Chem. 56 (2013) 1291–1300.

Please cite this article as: F. Caruso, et al., The in vitro antitumor activity of arene-ruthenium(II) curcuminoid complexes improves when decreasing curcumin polarity, J. Inorg. Biochem. (2016), http://dx.doi.org/10.1016/j.jinorgbio.2016.06.002